Journal of Applied Polymer Science

Modified Polyaniline and Its Effects on the Microstructure and Antistatic Properties of PP/PANI-APP/CPP Composites

Jing Xu, Jie Xiao, Zhiye Zhang, Xinlong Wang, Xiaodong Chen, Xiushan Yang, Wei Zhang, Lin Yang

College of Chemical Engineering of Sichuan University, Chengdu, Sichuan 610065, China
Correspondence to: L. Yang (E-mail: 18980632893@163.com)

ABSTRACT: Polypropylene (PP) composites that contain poly(aniline) (PANI) and ammonium polyphosphate crystalline form II (APP-II) have both antistatic and flame-retardant properties. In the present study, double anti-functional PANI was prepared via *in situ* polymerization in the presence of APP-II. Analysis of the Fourier transform infrared spectra demonstrated that PANI was synthesized successfully with APP-II and that modified PANI (PANI-APP) was obtained. Next, PP/PANI-APP/chlorinated poly(propylene) (CPP) and PP/PANI/CPP composites were prepared. The results showed that the volume resistivity of the PP/PANI-APP/CPP composite was at least 100 times less than that of the PP/PANI/CPP composite. The microstructures of the corresponding composites were investigated carefully by scanning electron microscopy and wide angle X-ray diffraction. The areas of the conductive regions and the percentage crystallinity of PP in the PP/PANI-APP/CPP composite were distinctly higher than those in the PP/PANI/CPP composite, i.e., by about 10% and 7%, respectively. In addition, experimental analyses of the limiting oxygen index and thermogravimetry showed that the PP/PANI-APP/CPP composite had advantages compared with PP in terms of its flame-retardant properties thermal stability. © 2014 Wiley Periodicals, Inc. J. Appl. Polym. Sci. **2014**, *131*, 40732.

KEYWORDS: blends; copolymers; electrospinning; flame retardance; structure-property relations

Received 7 January 2014; accepted 17 March 2014
DOI: 10.1002/app.40732

INTRODUCTION

Because of its superior mechanical and physiochemical properties, poly(propylene) (PP) is used in a wide variety of applications, such as the auto industry, electricity, engineering, housing materials, and transport.[1–4] However, PP is highly insulated and its chemical composition makes it flammable, which limit its range of application. Therefore, antistatic and flame retardant properties are essential requirements for improving PP.

Among the antistatic agents applied to PP, poly(aniline) (PANI) has the highest potential to become economically competitive, because it requires cheap materials and a simple synthesis method, while it also has good stability in the environment[5–7] and high electrical conductivity, which can be controlled reversibly by changing the oxidation state and protonation of the imine nitrogen groups.[8] In previous research, Yang et al.[9–12] showed that PANI is highly effective in enhancing the electrical properties of PP. The relationships between the electrical properties and the structures of PP/PANI/MWNT, PP/PANI/ PP/PANI-APP/chlorinated poly(propylene) (CPP), and PP/PANI/CPP-SO_3H composites were analyzed in detail. The volume resistivity of PP/PANI/CPP reached a peak of 3.89×10^{11} ohm cm^{-1} when the PANI content was 4.1%, while the volume conductivity of PP/PANI/MWNT-5, where the PANI-DBSA:MWNT ratio was 3 : 17, was the highest among all the composites.

Among the flame retardants used in PP, ammonium polyphosphate crystalline form II (APP-II) has attracted the greatest attention in recent years. It is more environmentally friendly[13–15] than traditional halogen-containing flame retardants and is more efficient as a flame retardant. For example, it tends to emit less smoke and fewer toxic gases during combustion, which conform to current developmental trends for flame retardants. In a previous study, Zhou et al.[16] reported the preparation of microencapsulated APP coated with melamine formaldehyde (MF) by in situ polymerization, where the limiting oxygen index (LOI) value reached 39.6 when the APP content was 30% and the composite passed the V-0 rating.

Previous researchers have mainly studied the antistatic or flame-retardant properties of PP composites. However, in many cases (such as in the coal, petroleum, chemical, rubber, paper printing, and powder processing industries), PP must possess antistatic and flame-retardant properties at the same time. To prepare double anti-functional materials, antistatic agents (for example PANI) and flame retardants (for example APP-II) must be added to PP composites simultaneously. The addition of an

Table I. Compositions of the PP/PANI/CPP and PP/PANI-APP/CPP Composites

Sample code	PP (g)	$PANI_{emer}$ (wt %)	PANI-DBSA/APP (wt %)	CPP (wt %)	Antioxidant (g)
PP/PANI/CPP[18]	87.2	4.1	0	13.2	0.9
PP/PANI-APP/CPP-1	65.6	3.9	10	13.0	0.7
PP/PANI-APP/CPP-2	61.6	5.8	15	13.0	0.6
PP/PANI-APP/CPP-3	57.6	7.7	20	13.0	0.6
PP/PANI-APP/CPP-4	53.6	9.6	25	13.0	0.5
PP/PANI-APP/CPP-5	49.6	11.6	30	13.0	0.5

antistatic agent and flame retardant are two relatively independent processes, which means that the production of double anti-functional materials is complex. Furthermore, the addition of double anti-functional materials weakens the mechanical properties of PP blends because the molar ratio of the fillers is very high in these blends. Therefore, it is necessary to perform in-depth studies of double-functional fillers with both antistatic and flame-retardant properties to simplify the preparation process, reduce the amount of fillers required, and reduce the degradation of the mechanical properties of the PP materials.

The present study investigated the production of modified PANI (PANI-APP) and determined the antistatic and flame-retardant performance of PP composites at the same time. Thus, the double anti-functional PANI was prepared via *in situ* polymerization in the presence of APP-II and we used the modified PANI to prepare PP/PANI-APP/CPP composites. The modified PANI was characterized based on its Fourier transform infrared spectra (FT-IR). The electric properties of PP/PANI-APP/CPP composites were measured using a high-resistance instrument. The flame retardancy and the microstructure of PP/PANI-APP/CPP composites were evaluated carefully based on the LOI, thermogravimetry (TG), scanning electron microscopy (SEM), and wide angle X-ray diffraction (WAXD).

EXPERIMENTAL

Materials

Aniline and hydrochloric acid (HCl) were provided by the Kelong Chemical Reagent Factory (Chengdu, China). PP (white powder, isotactic index = 96%, melt flow index = 3.5 g/10 min, apparent density = 0.43 g mL^{-1}) was provided by Kaikai Petroleum chemical company. Dodecylbenzene sulfonic acid (DBSA), aqueous ammonia ($NH_3{\cdot}H_2O$), and ammonium persulfate were supplied by Kewei Chemicals (China) and their contents were about 96 wt %. CPP was supplied by Sichuan Weiye Chemicals (China) and its chlorine content was about 31 wt %. APP-II (average degree of polymerization of ca 1000) was kindly donated by Shanghai Xushen Nonhalogen Smoke Suppressing Fire Retardants Co. Ltd. Deionized water was used in all preparations.

Preparation of PANI-APP

Fifty milliliters of HCl were mixed with 200 mL of deionized water in a beaker (500 mL) to obtain dilute hydrochloric acid. Next, 109.6 mL (0.6 mol) of aniline was added to the dilute hydrochloric acid to obtain the aniline acid solution. APP-II, 121.88 g (0.6 mol), was dissolved in a small amount of distilled water in a beaker (1000 mL) with vigorous stirring. The aniline acid solution was then added to the APP-II solution. Ammonium persulfate, 143.77g (0.63 mol), was dissolved in 300 mL of deionized water in a beaker (500 mL). The ammonium persulfate solution was then added slowly to the solution contained aniline and APP-II with a constant pressure funnel. The slurry obtained was maintained for 12 h in the mother liquid at 20°C with vigorous stirring. The slurry was then filtered to obtain the raw product, which was followed by several washes using the dispersion and filtration processes in distilled water. Next, the PANI-APP protonated with HCl (PANI-HCl/APP) was prepared.

PANI-HCl/APP was neutralized with 25 wt % $NH_3{\cdot}H_2O$ aqueous solution for 24 h, then filtered and washed with deionized water until the pH value of the percolate was 6 to 8. The polyemeraldine base ($PANI_{emer}$/APP) obtained was dried under vacuum. The purified and dried $PANI_{emer}$/APP was blended with dodecyl benzene sulphonic acid (DBSA), and the molar ratio of DBSA to $PANI_{emer}$/APP was 0.5. The blend was stirred for 48 h at ambient temperature, which yielded $PANI_{emer}$/APP protonated with DBSA (PANI-DBSA/APP).

Preparation of the PP/PANI-APP/CPP COMPOSITES

The total content of PP/PANI-APP/CPP composites was kept at about 80 g and PANI-APP was introduced into the PP/CPP at concentrations of 10 to 30 wt %. Composites of PP/CPP with different PANI-APP contents were prepared in a twin screw extruder at about 180°C. The mixed samples were hot-pressed at about 180°C under 10 MPa for 10 min to produce sheets of a suitable thickness, which were cooled to ambient temperature at a cooling rate of 30°C min^{-1} in the mold at 10 MPa.[17] The blend compositions and their sample codes are shown in Table I.

Measurements

Analysis of P_2O_5 Content. The P_2O_5 content was measured by a gravimetric method, i.e., HGT 2770-1996.

$$P_2O_5\% = \frac{(m_2 - m_1) \times 0.03207}{m} \times 100\%$$

where m_2 is the mass of the crucible and precipitate (the precipitate was obtained by a series of PANI-APP processing steps), m_1 is the mass of the empty crucible, and m is the mass of the PANI-APP.

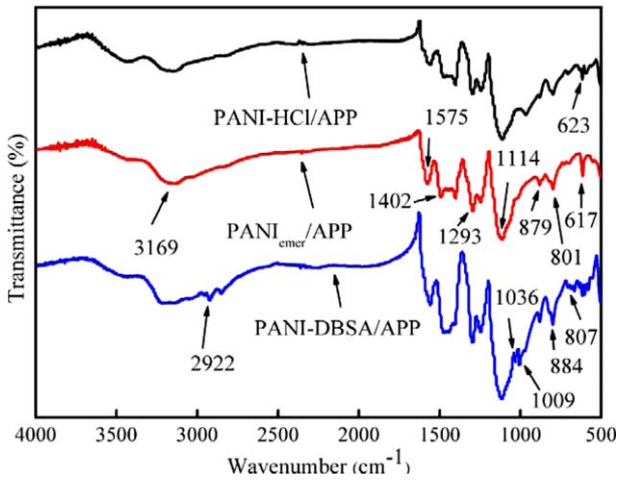

Figure 1. FT-IR spectra of PANI-HCl/APP, PANI$_{emer}$/APP, and PANI-DBSA/APP. [Color figure can be viewed in the online issue, which is available at wileyonlinelibrary.com.]

Fourier Transform-Infrared Spectra (FT-IR). All of the specimens analyzed by FT-IR were prepared as follows: powder samples were mixed with KBr powder and the mixture was pressed into a tablet. FT-IR analysis was conducted using a Nicolet 6700 spectrophotometer (Nicolet).

Limiting Oxygen Index (LOI). LOI was measured according to GB 2406.2-2009 (China) using an XZT-100A oxygen index meter (Kecheng, China).

Thermogravimetry (TG). TG analysis was performed using a TA Instruments NETZSCH TG 209 F1 Iris system (Germany). The samples were heated from room temperature to 550°C at a heating rate of 10°C min^{-1} in a nitrogen atmosphere with a flow rate of 10 mL min^{-1}.

Volume Resistivity. The volume resistivity of the composites was detected using a high resistance meter (ZC46A) produced by Shanghai Precision Scientific Instruments (China). The result obtained for each sample was the average of four measurements.

Scanning Electron Microscope (SEM). A JSM 5900 LV scanning electron microscope (SEM) was used to observe the morphology of the PP/PANI-APP/CPP composites. The samples were cut from 1 mm plates using a very sharp knife and then polished with a special polisher. The samples were then observed by SEM to determine the contrast between the electrically conductive and insulating regions of the material. The SEM images of the samples were not based on the actual material contrast, but instead they showed the contrast in the electrical conductivity between electrically conductive fillers and the insulating matrix.[18]

WAXD. The WAXD analyses were performed using a DX-2500 SSC diffractometer (China) in the reflection mode. Cu-Kα radiation was used at 20 kV and 40 mA. The analyses were performed at angles of 5 to 45° and the scan step was 0.052° (in 2θ) with a counting time of 20 s per step.

To determine the mass fraction of crystallinity, the WAXD curves were deconvoluted into crystalline and amorphous scattering components using the profile fitting program JADE6.5. Each peak was modeled using a Gaussian-Cauchy peak shape. The level of crystallinity was taken as the area ratio of all the crystalline peaks relative to that of the total scatter.

RESULTS AND DISCUSSION

FT-IR of PANI-APP-II

The FTIR spectra of PANI-HCl/APP, PANI$_{emer}$/APP, and PANI-DBSA/APP are shown in Figure 1. Clearly, the main absorption peaks of these three composites were around 3169 cm^{-1}, 1575 cm^{-1}, 1402 cm^{-1}, 1295 cm^{-1}, 1114 cm^{-1}, 879 cm^{-1}, 801 cm^{-1}, and 617 cm^{-1}. However, compared with PANI$_{emer}$/APP, the bands (879 cm^{-1}, 801 cm^{-1}, and 617 cm^{-1}) of PANI-HCl/APP and PANI-DBSA/APP had a slight red shift of about six wavenumbers, as shown in Figure 1. This was due to an enhancement of the oscillator strength of the backbone-related vibrations because of a vibronic coupling with the p-electron charge oscillation along the chain.[19] This indicates that the dedoping process of PANI$_{emer}$/APP was successful. Based on the main absorption peaks of PANI$_{emer}$/APP and PANI-DBSA/APP, the band at about 2900 cm^{-1} was produced by C-H, while the bands between 1050 and 1000 cm^{-1} were predominantly related to SO_2 and SO vibrations, which were attributable to the sulfonic group in DBSA.[20] However, these bands were not apparent in PANI$_{emer}$/APP. This demonstrated that the redoping process was achieved successfully. In general, comparisons of the FTIR spectra of PANI-HCl/APP, PANI$_{emer}$/APP, and PANI-DBSA/APP showed that the dedoping process and redoping process were achieved successfully. Thus, the double anti-functional PANI-APP was synthesized successfully.

Characterization of PP/PANI-APP/CPP Composites

Flame Retardancy of the Composites. LOI tests were conducted to evaluate the flame-retardant properties of the PP composites and the test results are shown in Table II. The LOI value of pure PP, which is a highly flammable polymeric material, was only 19. The LOI value of PP/PANI-APP/CPP-5 was 24.0, which shows that the introduction of PANI-APP can improve the LOI value of PP composites greatly. The LOI values of PP/PANI-APP/CPP composites increased with the PANI-APP content. This was probably because the modified PANI contained APP-II, which is a type of phosphorus flame retardant, and it improved the flame retardancy of PP/PANI-APP/CPP composites. PANI-APP and CPP increase the char formation capacity and they accelerated the char formation process during the combustion of PP/PANI-APP/CPP composites.

Table II. Flame Retardancy of Pure PP and PP/CPP/PANI-APP Composites

Sample code	LOI (%)
Pure PP	19
PP/PANI-APP/APP-1	21.0
PP/PANI-APP/CPP-2	22.0
PP/PANI-APP/CPP-3	22.1
PP/PANI-APP/CPP-4	22.3
PP/PANI-APP/CPP-5	24.0

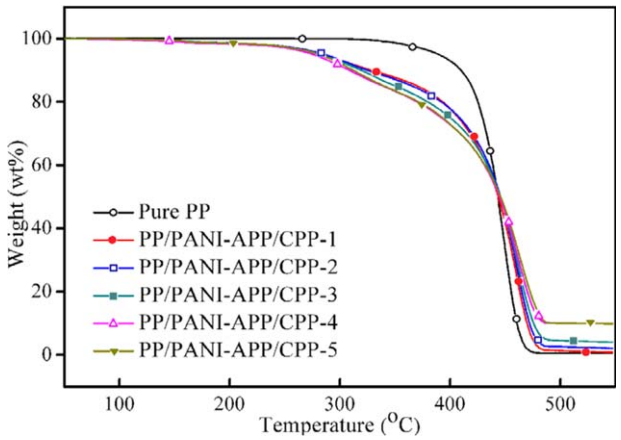

Figure 2. TG curves of (1) pure PP, (2) PP/PANI-APP/CPP-1, (3) PP/PANI-APP/CPP-2, (4) PP/PANI-APP/CPP-3, (5) PP/PANI-APP/CPP-4, and (6) PP/PANI-APP/CPP-5. [Color figure can be viewed in the online issue, which is available at wileyonlinelibrary.com.]

TG Analysis. Figures 2 and 3 show the TG and derivative thermogravimetric (DTG) curves of the pure PP and the PP/PANI-APP/CPP composites, respectively. The thermal degradation of the PP/PANI-APP/CPP composites comprised two main steps in a nitrogen atmosphere at about 310°C and 475°C. The first thermal degradation of PP/PANI-APP/CPP composites was attributed to the transformation of the crystal structure and the decomposition of APP-II. APP begins to decompose at about 200°C, forming phosphoric acid and liberating ammonia and H_2O.[16] The thermal degradation of pure PP has only one step. Compared with the second thermal degradation of PP/PANI-APP/CPP composites, it can be seen that the T_{onset}, T_{max}, and residue yield of pure PP were lower than that of the PP/PANI-APP/CPP composites.

Table III shows the T_{onset}, T_{max}, and residue yield values for the pure PP and PP/PANI-APP/CPP composites. Pure PP began to degrade at about 192°C (T_{onset}) and the PP/PANI-APP/CPP composites began to degrade at about 270°C. The T_{onset} of the PP/PANI-APP/CPP composites increased with the PANI-APP content. The T_{max} of pure PP was 460°C and the T_{max} of PP/PANI-APP/CPP composite was about 475°C. The T_{max} of PP/PANI-APP/CPP composites increased with the PANI-APP content. A comparison of the residue yield values of the pure PP and PP/PANI-APP/CPP composites showed that the residue yield of pure PP was only 0.65%, whereas the residue yields of the PP/PANI-APP/CPP composites were much higher. As shown in Table III, the addition of more PANI-APP to the PP/PANI-APP/CPP composites increased the amount of residual char in the PP/PANI-APP/CPP composites. There are several possible explanations for this result. In particular, the incombustible ammonia released via the thermal decomposition of APP-PANI may have diluted the air and simultaneously removed part of the heat generated during this process. Therefore, the PANI modified with APP-II is beneficial for increasing the amount of residual char and for improving the thermal stability of PP/PANI-APP/CPP composites.

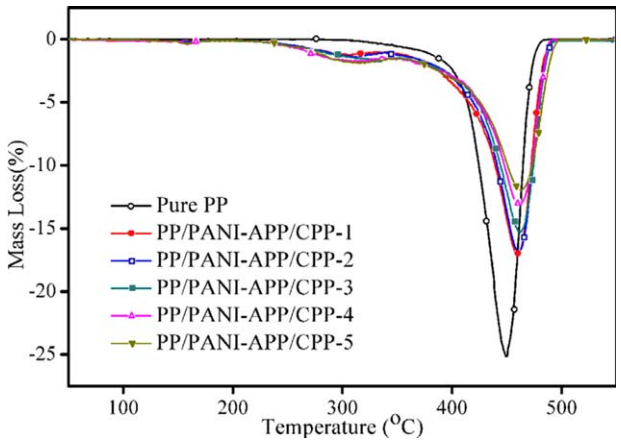

Figure 3. DTG curves of (1) pure PP, (2) PP/PANI-APP/CPP-1, (3) PP/PANI-APP/CPP-2, (4) PP/PANI-APP/CPP-3, (5) PP/PANI-APP/CPP-4, and (6) PP/PANI-APP/CPP-5. [Color figure can be viewed in the online issue, which is available at wileyonlinelibrary.com.]

Table III. Residual char, T_{onset}, and T_{max} of PP and PP/PANI-APP/CPP Composites

Sample code	T_{onset} (°C)	T_{max} (°C)	Residue yield (%)
Pure PP	191.9	462.8	0.65
PP/PANI-APP/CPP-1	266.4	473.7	0.80
PP/PANI-APP/CPP-2	270.3	475.0	2.09
PP/PANI-APP/CPP-3	273.3	477.0	4.01
PP/PANI-APP/CPP-4	268.7	477.1	9.83
PP/PANI-APP/CPP-5	278.8	480.2	9.83

T_{onset}: the actual temperature at which the weight loss rate began to grow rapidly; T_{max}: the actual temperature at which the maximum weight loss rate occurred.

Volume Resistivity of PP/PANI/CPP and PP/PANI-APP/CPP Composites. In this study, the phosphorus content was determined by analyzing the P_2O_5 content of the PANI-APP. In the PANI-APP composite, phosphorus was present only in the APP, so the $PANI_{emer}$ content of the PP composites could be obtained by eliminating the APP content from the PANI-APP. The $PANI_{emer}$ contents of the PP/PANI/CPP and PP/PANI-APP/

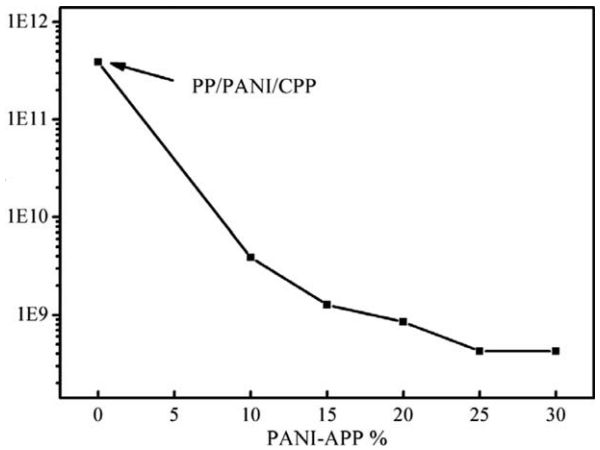

Figure 4. Relationship between the volume resistivity and PANI-APP content.

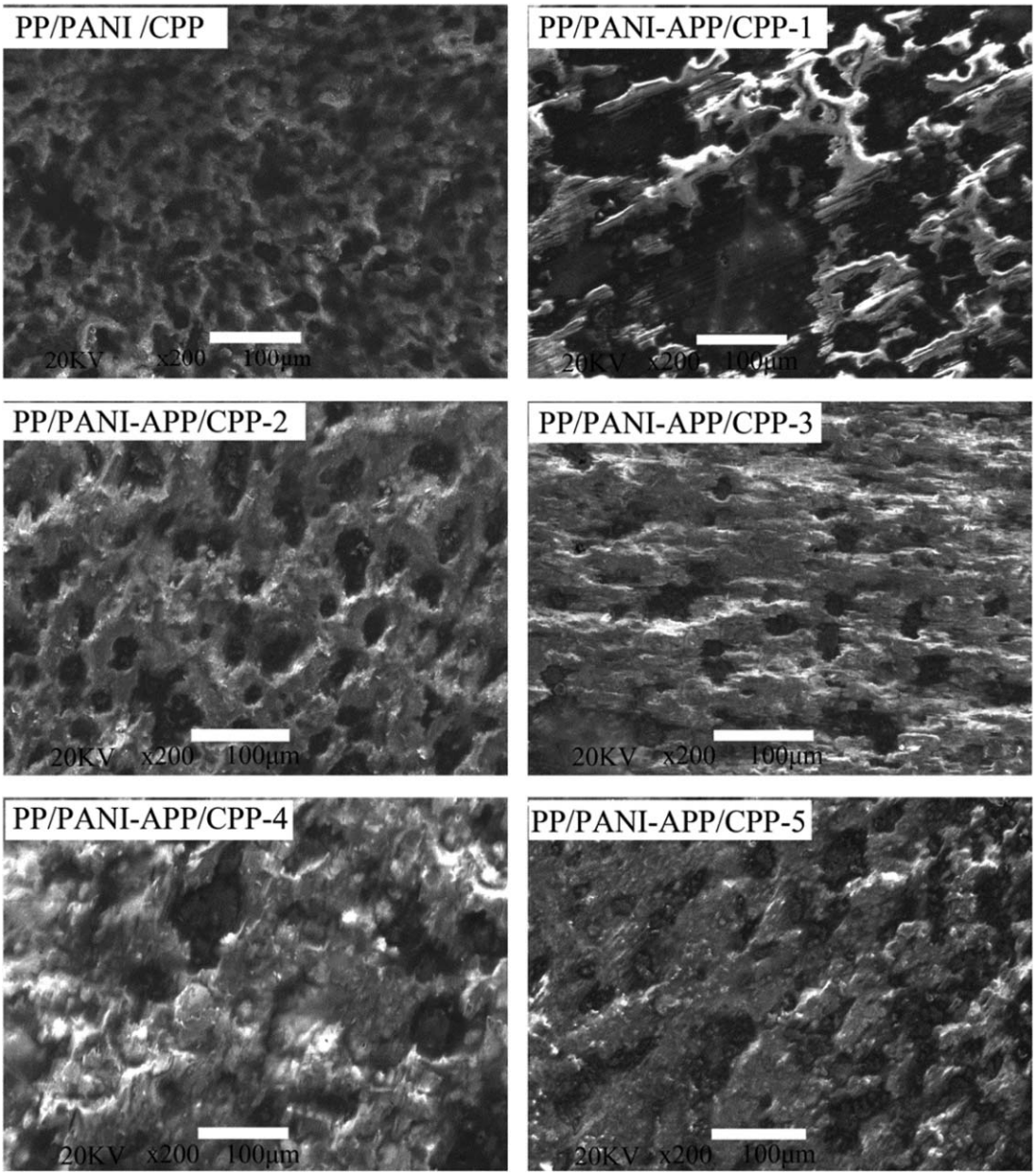

Figure 5. SEM micrographs of PP/PANI/CPP and PP/PANI-APP/CPP composites.

CPP composites are shown in Table I. Figure 4 shows the volume resistivity curves for the PP/PANI/CPP and PP/PANI-APP/CPP composites. According to Table I and Figure 4, the first point in the curve is PP/PANI/CPP with a $PANI_{emer}$ content of 4.1%. The other points are the PP/PANI-APP/CPP composites, where the $PANI_{emer}$ content of PP/PANI-APP/CPP-1 was 3.9%.

According to Yang et al., the addition of PANI improved the antistatic performance of PP composites in an effective manner. When the $PANI_{emer}$ and CPP contents were 4.1% and 13%, respectively, the volume resistivity reached a maximum of 3.89×10^{11} ohm cm^{-1},[9] which is the first point in the Figure 4. A comparison of the first and second points shows that when the $PANI_{emer}$ content of PP/PANI-APP/CPP-1 was less than that of PP/PANI/CPP, the volume resistivity value of PP/PANI/CPP was 3.89×10^{11} ohm cm^{-1}, whereas the volume resistivity of PP/PANI-APP/CPP-1 was lower at 3.89×10^{9} ohm cm^{-1}, i.e., 100 times less than that of PP/PANI/CPP. This indicated that the modified PANI was highly beneficial for reducing the volume resistivity of the PP/PANI-APP/CPP composites. These results may be explained by the modified PANI forming a shell on the surface of APP-II, which increased the contact surface of the PANI. This would have increased the dispersion effect of PANI in the composite material and increased the conducting area.

Figure 4 shows that the volume resistivity value decreased as the PANI-APP content increased until it reached a stable value. When the PANI-APP content was <15%, the volume resistivity value decreased rapidly with the increasing PANI-APP content,

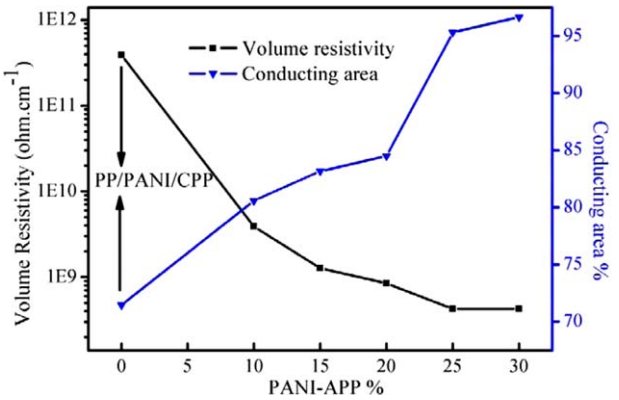

Figure 6. Relationships between the area of the conducting regions and the volume resistivity and PANI-APP content. [Color figure can be viewed in the online issue, which is available at wileyonlinelibrary.com.]

but this decline slowed as the PANI-APP content increased further When the PANI-APP content was >25%, the volume resistivity value reached a stable level. This may be because PANI-APP plays a role in compatibility and as a dispersing agent in the PP/PANI-APP/CPP composites, which makes the composites prone to conductance. When the PANI-APP content was superabundant, the compatibility and dispersion were limited.

Morphology of the Composites. Figure 5 shows SEM images of the PP/PANI-APP/CPP composites and PP/PANI/CPP. The first image in Figure 5 shows PP/PANI/CPP where the $PANI_{emer}$ content was 4.1%. The other images show PP/PANI-APP/CPP composites, where the $PANI_{emer}$ content in the PP/PANI-APP/CPP-1 was 3.9%. Before the SEM observations, the specimens were polished using a special polisher, so almost all of the pixels shown in Figure 6 lie on the same plane and there are no protuberant regions. Thus, the white parts can definitely be ascribed to the insulating regions (i.e., there was no PANI), whereas the black parts can be ascribed clearly to the conducting regions. The gray regions indicate transitions from insulating regions to conducting regions. PANI was also dispersed in the gray regions. The $PANI_{emer}$ content of the gray regions was lower than that of the black regions and the darker color indicates a higher $PANI_{emer}$ content. Therefore, PANI was dispersed in the gray and black regions, and the PANI dispersion properties were elucidated in PP/PANI-APP/CPP composites using this method.

Figure 5 shows that when the $PANI_{emer}$ content of PP/PANI-APP/CPP-1 was less than that of PP/PANI/CPP, the black regions of PP/PANI-APP/CPP-1 were more abundant than those of PP/PANI/CPP, which indicated that the conducting regions of PP/PANI-APP/CPP-1 were more abundant than those of PP/PANI/CPP. Therefore, the continuity of PANI in PP/PANI-APP/CPP-1 was better than that in PP/PANI/CPP. Thus, the electron conduction properties of PP/PANI-APP/CPP-1 were greater than those of PP/PANI/CPP, so the volume resistivity of PP/PANI-APP/CPP-1 was lower. As shown in Figure 5, the conducting regions of the PP/PANI-APP/CPP composites increased with the PANI-APP content. First, the continuity of PANI increased rapidly with the PANI-APP content, but it then increased slowly as the PANI-APP content increased further. When the PANI-APP content was >25% content, the continuity and the dispersion of PANI became fixed.

The intensity of white regions was defined as 255 and that of black regions was defined as 0 in the SEM images, so Figure 5 could be digitally analyzed. The total areas of the color intensity ranges were then statistically analyzed. Some gray regions had intensities of 150 to 255, but the ability of these gray regions to conduct electrons was very weak. Thus, to facilitate the statistical analysis, areas with an intensity of 0 to 135 were regarded as the conducting regions and those areas with an intensity of 150 to 255 were treated as the insulating regions. A color intensity range of 135 to 150 was very difficult to attribute to the conducting regions or the insulating regions, but this did not affect the trends in the areas of the conducting or insulating regions, which changed with the PANI-APP content. The area of each sample was calculated based on the average of three images.

Figure 6 shows the relationship between the area of the conducting regions and the change in the volume resistivity with the PANI-APP content. The relationship between the area of the conducting parts and the PANI-APP content was the opposite of that of the volume resistivity change with the PANI-APP content. When the $PANI_{emer}$ content of PP/PANI-APP/CPP-1 was less than that of PP/PANI/CPP, the area of the conducting regions in PP/PANI/CPP was 71%, whereas the area of the conducting regions in PP/PANI-APP/CPP-1 was 81%, i.e., more than that of PP/PANI/CPP. Therefore, the volume resistivity value of PP/PANI-APP/CPP-1 was at least 2 orders of magnitude lower than that of PP/PANI/CPP. This was possibly because the modified PANI formed a shell on the surface of APP, which increased the conductive contact surface of PANI. Therefore, when the $PANI_{emer}$ content was less than that of PP/PANI/CPP, the conductivity of PP/PANI-APP/CPP-1 was better than that of PP/PANI/CPP. Based on the PP/PANI-APP/CPP composites, the area of the conducting parts increased initially with the PANI-APP content when the PANI-APP content was

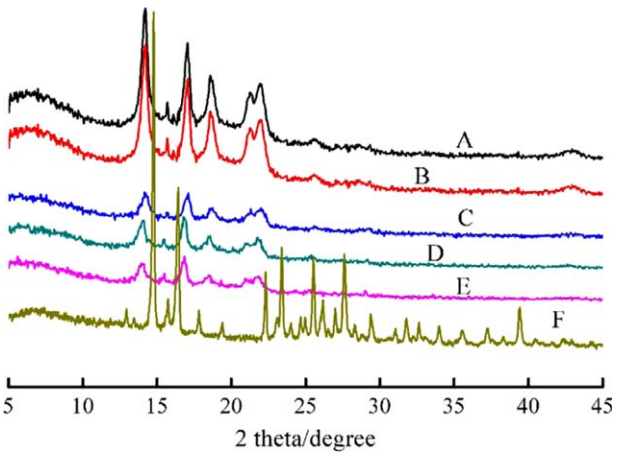

Figure 7. WAXD patterns of (A) PP/PANI-APP/CPP-1, (B) PP/PANI-APP/CPP-2, (C) PP/PANI-APP/CPP-3, (D) PP/PANI-APP/CPP-4, (E) PP/PANI-APP/CPP-5, and (F) pure APP in a range of 5 to 45°. [Color figure can be viewed in the online issue, which is available at wileyonlinelibrary.com.]

Table IV. Structural Parameters of PP/PANI/CPP and PP/PANI-APP/CPP Composites Based on WAXD Analysis

Sample code	Crystallinity of PP composite (%)	Crystallinity of PP (%)		A1	B	A2	A3	A4	A5
PP/PANI/CPP[18]	–	56.1	2θ(°)	13.96	15.59	16.81	18.42	20.94	21.71
			d(Å)	6.34	5.55	5.27	4.81	4.24	4.09
			FWHM	0.42	0.25	0.37	0.49	0.56	0.55
PP/PANI-APP/CPP-1	68.14	63.2	2θ(°)	14.17	15.64	17.04	18.65	21.28	21.93
			d(Å)	6.26	5.65	5.22	4.75	4.19	4.04
			FWHM	0.56	0.33	0.46	0.58	0.54	0.63
PP/PANI-APP/CPP-2	73.29	65.8	2θ(°)	14.02	15.54	16.88	18.51	21.10	21.18
			d(Å)	6.31	5.70	5.27	4.81	4.22	4.08
			FWHM	0.52	0.35	0.46	0.57	0.53	0.60
PP/PANI-APP/CPP-3	77.02	67.0	2θ(°)	14.21	15.74	17.06	18.69	21.26	21.95
			d(Å)	6.22	5.64	5.22	4.72	4.18	4.04
			FWHM	0.57	0.32	0.49	0.53	0.59	0.62
PP/PANI-APP/CPP-4	82.1	72.3	2θ(°)	13.99	15.47	16.83	18.52	20.07	21.82
			d(Å)	6.35	5.73	5.27	4.80	4.21	4.07
			FWHM	0.59	0.31	0.46	0.54	0.51	0.59
PP/PANI-APP/CPP-5	88.8	74.1	2θ(°)	13.95	15.42	16.81	18.44	21.06	21.79
			d(Å)	6.34	5.73	5.28	4.83	4.22	4.07
			FWHM	0.62	0.33	0.44	0.55	0.44	0.66

<25%, but it stabilized with further increases in the PANI-APP content. The trend in the change in the area of the conducting regions with the PANI-APP content reflected the change in the volume resistivity with the PANI-APP content.

WAXD Analysis. Figure 7 shows the WAXD patterns of pure APP-II and PP/PANI-APP/CPP composites over a range of 5 to 45°. PP and APP-II are crystallizable. PP has three types of crystalline phases: α-crystal, β-crystal, and γ-crystal. Figure 7 shows the presence of α-crystal (crystalline peaks at about 14°, 17°, 18.5°, 21°, and 21.8°) and β-crystal (crystalline peak at about 16°) components.[21]

To quantify the effect of the PANI-APP content on the crystal structure of PP in the PP/PANI-APP/CPP composites, WAXD curves were fitted using the profile fitting program JADE6.5. The fitting range was set at 10 to 26° because most of the crystalline peaks were within this range. Using Scherer's law and the mass fraction of crystal formula (i.e., % crystallinity = $A_c/(A_c + A_n)$, where A_c is the scattering from sharp crystalline area peaks and A_n is the scattering from noncrystalline areas), the percentage crystallinity of the PP/PANI-APP/CPP composites and pure APP-II were calculated.

The calculation showed that the percentage crystallinity of pure APP-II was about 97.9%. APP-II and PP were crystalline in the PP/PANI-APP/CPP composites, so each peak of the crystalline PP was very difficult to obtain. Thus, a simple method was used to determine the relative percentage crystallinity of PP according to the following equation:

$$\text{Crystallinity of PP \%} = \text{Crystallinity of composites \%} - \text{APP-II \%} \times 97.9\%$$

The profile fitting and calculation results for the WAXD curves of the PP/PANI-APP/CPP composites are shown in Table IV.

The data in Table IV represent the profile fitting results for the WAXD curves of the PP/PANI/CPP and PP/PANI-APP/CPP composites. The $PANI_{emer}$ content of PP/PANI/CPP was 4.1%, whereas the $PANI_{emer}$ content of PP/PANI-APP/CPP-1 was about 3.9%. A comparison between PP/PANI-APP/CPP-1 and PP/PANI/CPP showed that the interplanar distances of the PP crystals in each crystalline peak were similar. However, the percentage crystallinity of PP in PP/PANI-APP/CPP-1 was higher than that in PP/PANI/CPP. In the PP/PANI-APP/CPP composites, the interplanar distances of each crystalline peak were similar. The crystallinity of the PP crystals increased initially with the PANI-APP content, before reaching a stable value when the PANI-APP content was >25%.

Figure 8 shows plots of the volume resistivity and crystallinity for the PP/PANI/CPP and PP/PANI-APP/CPP composites. The first point

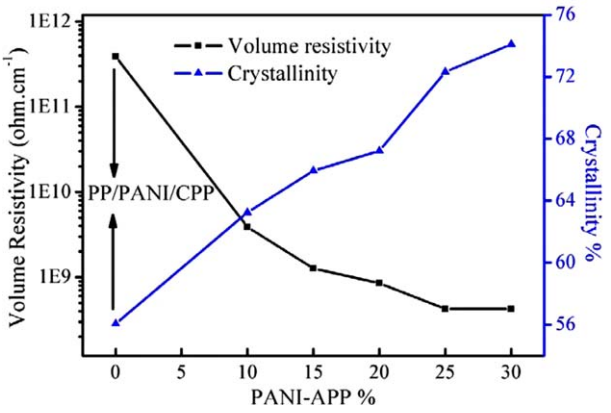

Figure 8. Volume resistivity and crystallinity *versus* PANI-APP content. [Color figure can be viewed in the online issue, which is available at wileyonlinelibrary.com.]

for PP/PANI/CPP occurred when the $PANI_{emer}$ content was 4.1%. The other points are the PP/PANI-APP/CPP composites when the $PANI_{emer}$ content of PP/PANI-APP/CPP-1 was about 3.9%.

A comparison of the first and second points shows that, although the $PANI_{emer}$ content of PP/PANI-APP/CPP-1 was less than that of PP/PANI/CPP, the crystallinity of PP/PANI/CPP was 56%, whereas the crystallinity of PP/PANI-APP/CPP-1 was 63%, i.e., much higher than that of PP/PANI/CPP. Thus, the volume resistivity of PP/PANI-APP/CPP-1 was lower than that of PP/PANI/CPP. Thus, PANI-APP may be beneficial for improving the crystallinity, for forming conductive pathways of PANI-APP in the PP/PANI-APP/CPP composites, and increasing the contact area, thereby decreasing the volume resistivity of the PP/PANI-APP/CPP composites. In the PP/PANI-APP/CPP composites, the crystallinity increased with the PANI-APP content, until it reached a stable level when the PANI-APP content was >25%. The trend in the crystallinity change reflected the change in the volume resistivity with the PANI-APP content.

CONCLUSIONS

The FT-IR results demonstrated that double anti-functional PANI was prepared successfully via *in situ* polymerization in the presence of APP-II. The LOI results showed that PANI-APP was conducive to improving the flame retardancy of PP/PANI-APP/CPP composites. The TG results showed that PANI-APP helped to increase the residual char amount and to enhance the thermal stability of PP/PANI-APP/CPP composites. When the $PANI_{emer}$ content of PP/PANI-APP/CPP-1 was less than that of PP/PANI/CPP, the volume resistivity of PP/PANI-APP/CPP-1 was at least two orders of magnitude less than that of PP/PANI/CPP. This result showed that the modified PANI was highly beneficial for reducing the volume resistivity of the PP/PANI-APP/CPP composites. The area of the conducting regions in PP/PANI-APP/CPP-1 was about 10% greater than that of PP/PANI/CPP. This was because the modified PANI formed a shell on the surface of APP, which increased the conductive contact surface of PANI. The percentage crystallinity of PP was about 7% higher than that of PP/PANI/CPP. PANI-APP was beneficial for improving the crystallinity and for forming conductive pathways of PANI-APP in the PP/PANI-APP/CPP composites. In the PP/PANI-APP/CPP composites, the volume resistivity decreased with the increasing PANI-APP content, whereas the area of the conducting regions and the percentage crystallinity of PP increased with the PANI-APP content, until they reached a stable level.

ACKNOWLEDGMENTS

This article is based on the results from the subject supported by National High Technology Research and Development Program of China (Grant No. 2011AA06A106) and Young Teachers Scientific Research Foundation Project of Sichuan University (2012SCU11024).

REFERENCES

1. Pandey, J. K.; Reddy, K. R.; Kumar, A. P.; Singh, R. P. *Polym. Degrad. Stab.* **2005**, *88*, 234.
2. Chem, X. L.; Yu, J.; He, M.; Guo, S. Y.; Luo, I.; Lu, S. J. *J. Polym. Res.* **2009**, *16*, 357.
3. Zhang, S.; Horrock, A. R. *Prog. Polym. Sci.* **2003**, *28*, 1517.
4. Chen, X.; Jiao, C. *Fire Safety J.* **2009**, *44*, 1010.
5. MacDiarmid, A. G. *Synth. Met* **1997**, *84*, 27.
6. Kim, B.; Koncar, V.; Devaux, E.; Dufour C. Viallier, P. *Synth. Met.* **2004**, *146*, 164.
7. Park, I. D.; Chang, D. H.; Kor. J. *Fiber. Soc.* **1996**, *33*, 17.
8. Barra, G. M. O.; Leyva, M. E.; Soares, B. G.; Mattoso, L. H.; Sens, M. *J. Appl. Polym. Sci.* **2001**, *82*, 114.
9. Yang, L.; Chen, J. Y.; Li, H. L. *J. Appl. Polym. Sci.* **2009**, *111*, 988.
10. Yang, L.; Zhang, Z. Y.; Wang, X. L.; Chen, J. Y.; Li, H. L. *Polym. J.* **2012**, *44*, 388.
11. Yang, L.; Chen, J. Y.; Li, H. L.; Zhang, Z. Y.; Wang, X. L. *Polym. Eng. Sci.* **2012**, *52*, 979.
12. Yang, L.; Zhang, Z. Y.; Wang, X. L.; Chen, J. Y.; Li, H. L.; *J. Appl. Polym. Sci.* **2013**, *128*, 1510.
13. Choi, Y. S.; Choi, S. K.; Moon, S. C.; Jo, B. W. *J. Ind. Eng. Chem.* **2008**, *14*, 387.
14. Liu, G. S.; Chen, W. Y.; Yu, J. G. *Ind. Eng. Chem. Res.* **2010**, *49*, 12148.
15. Lu, S, Y.; Hamerton, I. *Prog. Polym. Sci.* **2002**, *27*, 1661.
16. Zhou, J.; Yang, L.; Wang, X. L.; Fu, Q. J.; Sun, Q. L.; Zhang, Z. Y. *J. Appl. Polym. Sci.* **2013**, *129*, 36.
17. Yang, L.; Chen, J. Y.; Li, H. L. *Polym. Eng. Sci.* **2009**, *49*, 462.
18. Taipalus, R.; Harmia, T.; Zhang, M. Q.; Friedrich, K. *Compos. Sci. Technol.* **2001**, *61*, 801.
19. Huang, J.; Wan, M. X. *J. Polym. Sci.* **1999**, *37*,151.
20. Fryczkowski, R.; Biniaś, W.; Farana, J.; Fryczkowska, B.; Włochowicz, A. *Synth. Met.* **2004**, *145*, 195.
21. Obadal, M.; Cermak, R.; Stoklasa, K. *Macromol. Rapid Commun.* **2005**, *26*, 1253.
22. Fryczkowski, R.; Biniaś, W.; Farana, J.; Fryczkowska, B.; Włochowicz, A. *Synth. Met.* **2004**, *145*, 195.
23. Garcia, J. R.; Sanchez, J. L. A.; Silva, R. C. *J. Mater. Sci.* **2005**, *22*, 2461.
24. Zhou, S.; Song, L.; Wang, Z. Z.; Hu, Y.; Xing, W.Y. *Polym. Degrad. Stab.* **2008**, *93*, 1799.
25. Ke, C. H.; Li, J.; Fang, K. Y.; Zhu, Q. L.; Zhu, J.; Yan, Q.; Wang, Y. Z. *Polym. Degrad. Stab.* **2010**, *95*, 763.
26. Duquesne, S.; Bras, M. L.; Bourbigot, S.; Delobel, R.; Camino, G.; Eling, B.; Lindsay, C.; Roels, T.; Vezin, H. *J. Appl. Polym. Sci.* **2001**, *82*, 3262.